

Generic Contrast Agents

Our portfolio is growing to serve you better. Now you have a choice.



[VIEW CATALOG](#)

AJNR

Abnormal Blood Oxygen Level–Dependent Fluctuations in Focal Cortical Dysplasia and the Perilesional Zone: Initial Findings

L. Gupta, P.A.M. Hofman, R.M.H. Besseling, J.F.A. Jansen and W.H. Backes

This information is current as of May 11, 2025.

AJNR Am J Neuroradiol 2018, 39 (7) 1310-1315

doi: <https://doi.org/10.3174/ajnr.A5684>

<http://www.ajnr.org/content/39/7/1310>

Abnormal Blood Oxygen Level–Dependent Fluctuations in Focal Cortical Dysplasia and the Perilesional Zone: Initial Findings

 L. Gupta,  P.A.M. Hofman,  R.M.H. Besseling,  J.F.A. Jansen, and  W.H. Backes

ABSTRACT

BACKGROUND AND PURPOSE: Focal cortical dysplasia is a common cause of intractable epilepsy for which neurosurgery is an option. Delineations of a focal cortical dysplasia lesion on structural brain images may not necessarily reflect the functional borders of normal tissue. Our objective was to determine whether abnormalities in spontaneous blood oxygen level–dependent fluctuations arise in focal cortical dysplasia lesions and proximal regions.

MATERIALS AND METHODS: Fourteen patients with focal cortical dysplasia–related epilepsy and 16 healthy controls underwent structural and resting-state functional MR imaging. Three known blood oxygen level–dependent measures were determined, including the fractional amplitude of low-frequency fluctuations, regional homogeneity, and wavelet entropy. These measures were evaluated in the lesion and perilesional zone and normalized to the contralateral cortex of patients with focal cortical dysplasia and healthy controls.

RESULTS: Patients showed significantly decreased fractional amplitude of low-frequency fluctuations and increased wavelet entropy in the focal cortical dysplasia lesion and the perilesional zone (≤ 2 cm) relative to the contralateral homotopic cortex and the same regions in healthy controls. Regional homogeneity was significantly increased in the focal cortical dysplasia lesion compared with the contralateral homotopic cortex and healthy controls.

CONCLUSIONS: Abnormalities in spontaneous blood oxygen level–dependent fluctuations were seen up to 2 cm distant from the radiologically visible boundary. It was demonstrated that functional boundaries go beyond structural boundaries of focal cortical dysplasia lesions. Validation is required to reveal whether this information is valuable for surgical planning and outcome evaluation of focal cortical dysplasia lesions and comparing current results with electrophysiologic analysis.

ABBREVIATIONS: BOLD = blood oxygen level–dependent; EEG = electroencephalography; fALFF = fractional amplitude of low-frequency fluctuations; FCD = focal cortical dysplasia; ReHo = regional homogeneity; WE = wavelet entropy

A focal cortical dysplasia (FCD) is a congenital malformation of cortical development and a frequent cause of intractable epilepsy in children and adults.¹ A complete resection of the epileptogenic zone is required to become seizure-free; therefore, an accurate visualization by neuroimaging is crucial for surgical planning. Histopathologic examination of surgical specimens has

demonstrated that 80% of patients who had a complete resection become seizure-free, compared with only 20% who had incomplete resections.² The most frequently mentioned cause of unsuccessful surgical treatment is invisibility of lesion boundaries on imaging modalities.³

The computer-aided diagnostic approach using morphologic characteristics such as focal cortical thickening or thinning, areas of focal brain atrophy, gray-white junction blurring, and increased signal on T2- and fluid-attenuated inversion recovery–weighted images assists in improving lesion detection.⁴ However, where the exact borders reside and whether the lesion and the perilesional zone are functionally normal or abnormal often remains unknown.^{5,6} Therefore, we proposed exploring a physiologic image contrast in FCD, in addition to the clinically used morphologic contrasts.

Simultaneous electroencephalography (EEG)-fMRI studies revealed that interictal epileptiform discharge–related hemodynamic changes were observed beyond the visible lesion on struc-

Received August 31, 2017; accepted after revision April 1, 2018.

From the Department of Radiology and Nuclear Medicine (L.G., P.A.M.H., R.M.H.B., J.F.A.J., W.H.B.) and School for Mental Health and Neuroscience (P.A.M.H., J.F.A.J., W.H.B.), Maastricht University Medical Center, Maastricht, the Netherlands; and Department of Electrical Engineering (R.M.H.B.), Eindhoven University of Technology, Eindhoven, the Netherlands.

This work was partly supported by a grant from the Dutch National Epilepsy Fund 10–08, and the study is registered in the Dutch Trial Registry (<http://www.trialregister.nl/trialreg/admin/rctview.asp?TC=2315>).

Please address correspondence to Walter H. Backes, PhD, Departments of Radiology and Nuclear Medicine, Maastricht University Medical Center (MUMC+), P.O. Box 5800, 6202 AZ Maastricht, the Netherlands; e-mail: w.backes@mumc.nl

<http://dx.doi.org/10.3174/ajnr.A5684>

Table 1: Patient characteristics

No.	Age/Sex	Seizure Frequency ^a	FCD Location	MRI Structural Image Findings
1	30/F	High	Right insula	Transmantle sign, gray-white matter blurring, cortical thickening, T2-FLAIR hyperintensity
2	29/F	High	Right superior frontal	Transmantle sign, gray-white matter blurring, cortical thickening, T2-FLAIR hyperintensity
3	33/M	Low	Right inferior frontal	Transmantle sign, gray-white matter blurring, T2-FLAIR hyperintensity
4	47/F	High	Right precentral	Transmantle sign, gray-white matter blurring, T2-FLAIR hyperintensity
5	21/M	Low	Left postcentral	Gray-white matter blurring, cortical thickening, T2-FLAIR hyperintensity
6	47/M	High	Left posterior cingulate	Transmantle sign, gray-white matter blurring, cortical thickening, T2-FLAIR hyperintensity
7	43/M	High	Left caudal middle frontal	Transmantle sign, gray-white matter blurring, cortical thickening, T2-FLAIR hyperintensity
8	26/M	Low	Left rostral middle frontal	Transmantle sign, gray-white matter blurring, cortical thickening, T2-FLAIR hyperintensity
9	21/F	Low	Caudal anterior cingulate	Transmantle sign, gray-white matter blurring, cortical thickening, T2-FLAIR hyperintensity
10	21/M	High	Right supramarginal	Transmantle sign, gray-white matter blurring, cortical thickening, T2-FLAIR hyperintensity
11	21/M	Low	Right insular	Transmantle sign, gray-white matter blurring, cortical thickening, T2-FLAIR hyperintensity
12	27/M	Low	Left precentral	Transmantle sign, gray-white matter blurring, cortical thickening, T2-FLAIR hyperintensity
13	54/M	High	Right rostral middle frontal	Transmantle sign, gray-white matter blurring, cortical thickening, T2-FLAIR hyperintensity
14	25/M	None	Left inferior parietal	Gray-white matter blurring, cortical thickening, T2-FLAIR hyperintensity

^a Seizure frequency: low, 1 per month; high, >1 per week.

tural MR imaging, and surgical outcomes were better using EEG-fMRI in addition to structural MR imaging and intracranial EEG.⁷ Electrophysiologic examinations have revealed epileptogenicity, not only in the lesion but also in perilesional areas.⁸ To our knowledge, no systematic imaging study has explored the physiology of the immediate vicinity of FCDs, which may be relevant for resection planning and outcome prediction.

Using resting-state functional MR imaging, we assessed the time signature of spontaneous blood oxygen level–dependent (BOLD) fluctuations in patients with FCD. We evaluated 3 known BOLD measures to characterize the spontaneous fluctuations: 1) the amplitude (fractional amplitude of low frequency fluctuations [fALFF]) as a measure of oscillation strength, 2) regional homogeneity (ReHo) as a measure of local signal similarity, and 3) wavelet entropy (WE) as a measure of disorder/order in BOLD time-series.

The same functional MR imaging dataset was previously used to show abnormalities in the spatial profile of functional connectivity of FCDs beyond the MR imaging–visible lesion.⁹ That study used a seed-based functional connectivity approach to determine the interregional correlations with remote brain regions, whereas in the current study, we characterized the intrinsic BOLD fluctuations in FCD lesions with local spatiotemporal measures (fALFF, ReHo, and WE). The objective of this study was to determine whether functional abnormalities arise in spontaneous BOLD fluctuations of FCD lesions and proximal regions in comparison with normal-appearing brain tissue.

MATERIALS AND METHODS

Subjects

The study was approved by the ethics committees of the 2 participating medical institutions. Informed written consent was obtained from all subjects. Fourteen patients with FCD-related epi-

lepsy were recruited (mean age, 32 ± 11 years; 10 men), as well as 16 age- and sex-matched healthy controls (mean age, 35 ± 9 years; 7 men). Structural MR images were rated by neuroradiologists with >20 years of experience. The clinical diagnosis was based on concordance among seizure semiology, EEG findings, and neuroimaging.¹ Briefly, this involved recurrent stereotyped seizures and focal interictal and/or ictal EEG abnormalities that coincided with an FCD-concordant lesion on MR imaging.¹⁰ Relevant imaging features included, among others, an abnormal gyral pattern, increased cortical thickness, the transmantle sign, and blurring of the gray-white matter interface.¹¹ None of the patients included in this study had dual pathology. Table 1 lists the lesion characteristics per patient. For 5 patients, surgery and histopathology information were also available, which further confirmed the diagnosis of FCD.

MR Imaging

All subjects underwent structural and functional MR imaging at 3T (Achieva; Philips Healthcare, Best, the Netherlands) using an 8-element receive-only head coil. Structural imaging involved a T1-weighted scan: 3D fast spoiled gradient-echo sequence; TE/TR/TI, 3.8/8.3/1022 milliseconds; voxel size, $1 \times 1 \times 1$ mm³; duration, 7.5 minutes. In addition, a FLAIR sequence was used (3D turbo spin-echo; TE/TR/TI, 330/8000/2400 milliseconds; 0.4×0.4 mm² pixel size; 0.6-mm-thick axial slices; duration, 8 minutes). Functional MR imaging involved a BOLD T2*-weighted task-free scan, for which the participants were instructed to close their eyes, lie still, and think of nothing in particular. The settings were the following: single-shot echo-planar imaging sequence; TE/TR, 35/2000 milliseconds; 2×2 mm² pixel size; 4-mm thick axial slices; 195 dynamics; duration, 6.5 minutes.

Image Processing

Functional images were corrected for slice-timing differences and head displacements, coregistered to the anatomic template, and smoothed with an 8-mm kernel (full width at half maximum) using computational software (Statistical Parametric Mapping, SPM8; <http://www.fil.ion.ucl.ac.uk/spm/software/spm12>). Any signal drifts across time were corrected by removing the very-low-frequency components (<10 MHz) (FSL 3.0; <http://www.fmrib.ox.ac.uk/fsl>). To correct for physiologic fluctuations, we included the time-series from the CSF and white matter as covariates in the linear regression analysis.¹² Gray matter, white matter, and CSF voxels were segmented from the T1-weighted images (FreeSurfer software, Version 5.3.0; <http://surfer.nmr.mgh.harvard.edu>).

Fractional Amplitude of Low-Frequency Fluctuations

The signal time-series of each voxel was standardized and Fourier-transformed to the frequency domain, and the power spectrum was calculated in specific frequency sub-bands. The fALFF is computed per voxel as the ratio of the power spectrum in a specific sub-band (10–80 MHz) to the full range (0–250 MHz)¹³ (Resting-State fMRI Data Analysis Toolkit [REST], Version 1.8; <http://www.rfmri.org/REST>). This ratio helps to eliminate the confounding influence of the relatively strong signal of the pulsating CSF and physiologic noise.¹³ The fALFF was computed in 4 predefined frequency sub-bands: 10–27 MHz (slow-5), 27–73 MHz (slow-4), 73–198 MHz (slow-3), and 198–250 MHz (slow-2).¹⁴

Regional Homogeneity

The Kendall coefficient of concordance was used to calculate the ReHo of the time-series of a voxel with its 26 (immediate) neighbor voxels (REST Toolkit, Version 1.8) as proposed by Zang et al.¹⁵

ReHo measures the similarity in contiguous voxels of the time-series and was averaged over all gray matter voxels per ROI. While most functional imaging analysis methods rely on a priori knowledge of a signal model, ReHo is a voxel-by-voxel, data-driven approach that requires no prior knowledge of the experimental design.

Wavelet Entropy

The wavelet entropy is computed using the discrete wavelet transform of the time-series.¹⁶ Unlike the Fourier transform or short-time Fourier transform, the nonstationary components in the BOLD time-series are detected by the discrete wavelet transform (Daubechies-4 wavelet) by means of the convolution with the time-shifted and scaled mother wavelet function. The resulting sub-bands are squared and integrated across time to obtain the energy E_i per sub-band i , from which the WE over the sub-bands is calculated as $WE = -\sum p_i \ln p_i$, with $p_i = E_i / \sum E_i$, the relative energy per sub-band. WE is a measure of lack of structure, thus randomness, over the wavelet sub-band. A typical BOLD signal represents a frequency structure in which the energy roughly decreases as a function of frequency (sub-band) due to the low-pass nature of the blood signal. When the distribution of energy over frequency sub-bands becomes more equal (ie, more random), WE increases.¹⁷

Image Analysis

FCDs were manually marked on the structural images by an experienced neuroradiologist on FLAIR images. These ROIs were spatially transformed to the functional images. Three proximal regions of FCD were selected at a 1-, 2-, and 3-cm distance from the lesion border, as 1-cm-thick shells. To reduce physiologic variation, we used the entire normal-appearing cortex of the contralateral hemisphere for normalizing all BOLD measures. In healthy controls, the BOLD measures were obtained from the anatomic atlas regions that spatially corresponded to the lesions in patients (using FreeSurfer software).

Statistical Analysis

Region-averaged BOLD measures of the FCD lesions and the homotopic contralateral cortex were reported as absolute (ie, not normalized to the contralateral cortex) values. In addition, normalized values were given as a ratio between the region-averaged BOLD value (fALFF, ReHo, or WE) and the mean measure of all voxels in the entire normal-appearing cortex of the contralateral hemisphere.

The Student 2-sample t test was used to reveal any differences between the patients with FCD and control subjects. The paired t test was used for statistical assessment of the FCD region, proximal regions, and contralateral homotopic cortex. Statistical significance was inferred at $P < .05$.

A threshold was derived from the results of the healthy control group (reference value). This threshold served to determine which and how many patients had abnormal BOLD values (ie, beyond the 95% confidence intervals of the healthy control group) in the lesion and proximal regions.

RESULTS

Figure 1 shows an FCD lesion on a FLAIR image with cortical maps of fALFF, ReHo, and WE of the FCD lesion and proximal cortex. In this example, decreased fALFF, increased ReHo, and increased WE were observed in the FCD lesion and the proximal regions.

Absolute BOLD Measures

Table 2 lists the absolute BOLD measures. The fALFF of the FCD lesions was significantly lower and wavelet entropy was significantly higher than the contralateral homotopic cortex and the same region in the control subjects. ReHo showed no significant differences.

Normalized Fractional Amplitude of Low-Frequency Fluctuations

Figure 2 provides the fALFF as a function of frequency in the range of 10–250 MHz for the FCD lesion, proximal regions, and controls. Only for the slow-5 sub-band (10–27 MHz) was the amplitude of the FCD lesions significantly lower than for the control subjects ($P < .001$). For this sub-band, all 3 proximal regions showed lower amplitudes than in controls. The most distant shell at 3 cm showed a significantly higher fALFF than the more proximal regions (1 and 2 cm).

Patients showed a significantly lower normalized fALFF in the FCD lesion and the closer proximal regions (at 1 and 2 cm) rela-

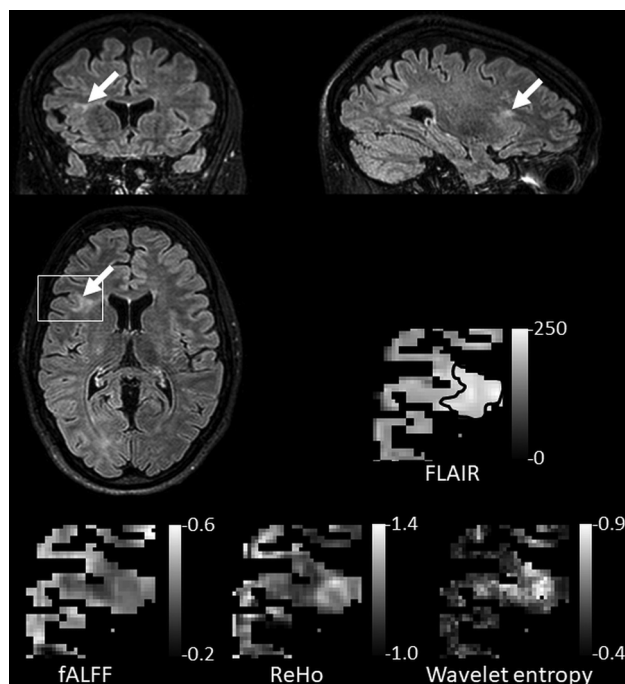


FIG 1. Sample orthogonal FLAIR images depicting an FCD lesion (arrows) of a 30-year-old woman. Inserts show the magnification of the lesion on FLAIR contrast and cortical parameter maps of fALFF, regional homogeneity, and wavelet entropy. Increased regional homogeneity, wavelet entropy, and decreased fALFF were observed in the FCD lesion and the immediate perilesional regions in comparison with the regions more distinct from the FCD. Only gray matter is visualized; white matter is masked out.

Table 2: Absolute BOLD measures in the FCD lesion, the contralateral homotopic cortex, and healthy controls^a

Absolute Measure	Lesion	Contralateral Homotopic Cortex	Controls
fALFF	0.327 ± 0.007 ^b	0.352 ± 0.008	0.358 ± 0.008
ReHo	0.348 ± 0.032	0.292 ± 0.031	0.310 ± 0.024
WE	1.245 ± 0.005 ^b	1.227 ± 0.004	1.227 ± 0.003

^a Data are mean ± standard error.

^b Significant differences ($P < .05$) with the contralateral homotopic cortex and the same region in controls, respectively.

tive to the contralateral homotopic cortex (FCD lesion: $P < .001$; proximal at 1 and 2 cm: $P < .02$) and the same regions in the control subjects (FCD lesion: $P < .001$; proximal at 1 and 2 cm: $P < .01$) (Table 3). Thirteen of 14 patients showed abnormal (lower) fALFF in the lesions, and 11 of these 13 patients showed abnormal fALFF up to 2 cm from the boundary (Table 4). Six patients showed abnormal fALFF in the contralateral homotopic cortex.

Normalized Regional Homogeneity

The normalized ReHo was significantly higher in FCD lesions compared with the contralateral homotopic cortex in patients ($P < .01$) and control subjects ($P < .01$). None of the proximal regions showed significant differences. The mean ReHo increased with the distance in the proximal regions (Table 3). Eleven of 14 patients showed abnormal (higher) ReHo in the lesion, and 5 of these patients showed abnormal ReHo up to 2 cm from the

boundary (Table 4). Four patients showed abnormal fALFF in the contralateral homotopic cortex.

Normalized Wavelet Entropy

The normalized WE for the FCD lesion and the closer proximal regions (at 1 or 2 cm) was significantly higher than the contralateral homotopic cortex (FCD lesion: $P < .01$; proximal at 1 and 2 cm: $P < .05$) and the same region in healthy controls (FCD lesion: $P < .01$; proximal at 1 and 2 cm: $P < .05$) (Table 3). Twelve of 14 patients showed abnormal (higher) WE in the lesion, and 10 of these patients showed abnormal WE up to 2 cm from the boundary (Table 4). Five patients showed abnormal WE in the contralateral homotopic cortex.

DISCUSSION

In this study, we set out to determine physiologic abnormalities of the BOLD signal time-series in FCD lesions of patients with epilepsy. The most suitable BOLD measures were obtained by normalizing lesion or perilesional values to the contralateral homotopic cortex. Patients with FCD showed significantly decreased oscillation amplitudes (normalized fALFF), decreased spatiotemporal heterogeneity (ie, increased normalized ReHo), and increased temporal heterogeneity (ie, increased normalized WE) in the FCD lesions compared with healthy controls. The most striking result was that abnormal BOLD fluctuations were also manifest in regions adjacent to the structurally visible borders of the lesions.

BOLD Abnormalities in FCD Lesions

Decreased BOLD amplitude (normalized fALFF) and increased temporal heterogeneity (increased normalized WE) suggest reduced neuronal activity or neurovascular coupling in the lesions. Suppression of activity in the FCD lesion was also previously reported in the intracranial EEG, where interrupted pseudoperiodic spikes were reported.¹⁸

There was also significantly increased normalized ReHo observed in patients with FCD lesions relative to healthy controls. This could be due to the lower amplitude, which also attenuates differences and randomness in BOLD signals within FCD lesions. The increase in normalized ReHo increases the similarity of the signals and thus increases ReHo.

Perilesional Functional Abnormalities

All 3 BOLD measures and the wavelet spectrum showed that the abnormalities extend beyond the visible lesion border on FLAIR images. An increase in normalized WE in the FCD lesion and the 2-cm perilesional zone was observed, indicating a more equalized frequency distribution over the sub-bands for the FCD lesion and the perilesional zone, which implies a less pronounced frequency structure. The normalized fALFF measure also showed reduction of activity, indicating that irregularities of the BOLD fluctuations in the perilesional zone may be related to some form of epilepsy-related activity of the impaired brain.^{7,19} However, from the current observations in patients with epilepsy, who were well-treated by medication and/or surgery, we cannot infer whether the perilesional activity acts as an epileptogenic or inhibitory mechanism.

Also previous electrophysiologic investigations showed that interictal epileptic discharges extend beyond the FCD visible le-

sion (ie, in perilesional regions).^{20,21} Urrestarazu et al²² reported that a very high rate of fast ripples in the EEG signal was observed in the perilesional area, which was adjacent to the seizure-onset area. The fast ripples in the perilesional zone might be an indicator of potential epileptogenicity, which Cohen-Gadol et al²³ suggested could possibly turn into a seizure focus after the removal of the primary seizure-onset zone. Other studies further suggested that removal of the entire lesion, including surrounding interictally active tissue, would be necessary to achieve long-term seizure relief.^{24,25}

The results indicated variability among patients because not all patients showed BOLD abnormalities up to 2 cm from the lesion boundaries and only a few patients showed abnormalities beyond 2 cm. This intersubject variation suggests that different pathologic mechanisms might be at work; for instance, excitotoxic effects could lead to variations in the BOLD signal. The variable findings may also reflect the heterogeneity of a clinical sample of patients with FCD, with variations in the frequency of epileptiform discharges and antiepileptic drug use. The results presented in this study are in line with the findings presented in a functional connectivity study, in which 11/14 patients (a similar number of patients showed abnormality using normalized fALFF and normalized WE) showed abnormality in FCD perilesional regions⁹ on the same dataset.

Note that because structural findings like the transmantle sign and gray-white matter blurring potentially infer an indeterminate lesion border, which may influence the exact values of the BOLD measures we obtained in individuals. In this study, we delineated

the lesion border on the hyperintensities of the FLAIR images, which were present for all subjects. It is unlikely that individual uncertainties in border definition would strongly influence our results because we present group average results.

Clinical Perspective

The most interesting finding of this study is that structural boundaries are not the same as functional boundaries obtained by the physiologic BOLD contrast for the FCD lesions. Reports indicate that on average, 62% of patients with cortical dysplasia are seizure-free after an operation.^{2,26} Our findings show that functional abnormalities, derived from spontaneous BOLD fluctuations, were seen up to 2 cm distant from the radiologically visible boundary of the FCD lesion. These findings could be critical information for surgery planning of FCD lesions.

Recent findings show that removing as much as possible of the aberrant cortex improves seizure-free outcome.² The presented BOLD method can possibly be used to help noninvasively assess the functional extent of FCD lesions and has the potential to unveil lesion areas that could be missed by structural MR imaging in a surgical work-up.

Study Considerations

Because the 2 brain hemispheres are intrinsically connected, the BOLD signal of the contralateral homotopic cortex is also likely to be affected by the abnormality caused by FCD. This abnormality was noticed because some patients showed increased normalized WE and decreased normalized fALFF in comparison with controls in the contralateral homotopic cortex.

Functional imaging has been linked to electrophysiology, in a previous study in which epileptiform spikes were mapped to the brain using simultaneously acquired EEG-fMRI.⁷ The current study results need to be verified by comparing BOLD measures on functional MR imaging data from patients who become seizure-free after an operation with measures of those who have recurrent seizures. Ideally, this comparison should be supplemented with histopathology according to the most recent classification,^{1,27} which we could not fully provide. Similarly, our findings on the abnormal BOLD fluctuations in the perilesional zone need to be evaluated against intracranial EEG recordings in suitable patient groups.

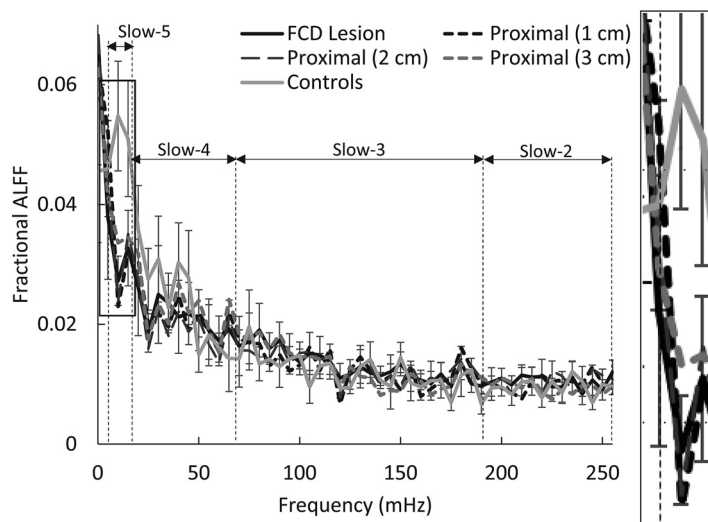


FIG 2. Fractional amplitude of low frequency fluctuations as a function of frequency in the range of 10–250 MHz. Only the lowest sub-band (ie, slow-5; 10–27 MHz, magnified) showed significantly lower amplitudes in the FCD lesion relative to the controls. Error bars represent the standard error of mean.

Table 3: The normalized BOLD measures in the FCD lesion, perilesional regions, contralateral homotopic region, and healthy controls^a

Normalized Measure	Lesion	Perilesional Zones			Contralateral Homotopic	Control Subjects
		1 cm	2 cm	3 cm		
fALFF	0.922 ± 0.016 ^b	0.941 ± 0.014 ^b	0.947 ± 0.014 ^b	0.981 ± 0.013	0.983 ± 0.012	1.005 ± 0.009
ReHo	1.206 ± 0.066 ^b	0.992 ± 0.032	0.991 ± 0.036	1.021 ± 0.034	1.023 ± 0.032	1.020 ± 0.022
WE	1.018 ± 0.004 ^b	1.013 ± 0.003 ^b	1.009 ± 0.003 ^b	1.003 ± 0.003	1.003 ± 0.002	1.002 ± 0.002

^a Data are mean ± standard error. Normalized fALFF was significantly decreased, while WE was significantly higher in FCD lesions and perilesional zones (up to 2 cm) than in the contralateral homotopic cortex and control subjects. ReHo was significantly higher in FCD lesions. BOLD measures were normalized with the entire contralateral cortex.

^b Significant differences ($P < .05$) with the contralateral homotopic cortex and the same region in controls, respectively.

Table 4: Number of patients with measures outside the 95% confidence interval of the normative (healthy control) values^a

Normalized Measure	Lesion	Perilesional Zone			Contralateral Homotopic Cortex
		1 cm	2 cm	3 cm	
fALFF	13 (93)	12 (86)	11 (79)	6 (43)	6 (43)
ReHo	11 (79)	5 (36)	5 (36)	4 (29)	4 (29)
WE	12 (86)	11 (79)	10 (71)	4 (29)	5 (36)

^a Data are the number of patients (percentage).

CONCLUSIONS

In this study, it was shown that functional boundaries of FCD extend beyond boundaries visible on structural MR imaging. Our findings show that functional abnormalities, in terms of attenuated and more disordered BOLD fluctuations, were seen up to 2 cm away from the radiologically visible boundary of the lesion. This information could be critical for surgery planning of FCD lesions, which needs to be validated with intracranial EEG recordings, because BOLD findings in the lesional and perilesional areas could reflect metabolic/hemodynamic changes due to epileptic discharges.

Disclosures: Paul A.M. Hofman—RELATED: Grant: Dutch Epilepsy Fund, Comments: Project 10–8.* *Money paid to the institution.

REFERENCES

- Blümcke I, Thom M, Aronica E, et al. The clinicopathological spectrum of focal cortical dysplasias: a consensus classification proposed by an ad hoc Task Force of the ILAE Diagnostic Methods Commission. *Epilepsia* 2011;52:158–74 CrossRef Medline
- Hauptman JS, Mathern GW. Surgical treatment of epilepsy associated with cortical dysplasia: 2012 update. *Epilepsia* 2012;53(Suppl 4):98–104 CrossRef Medline
- Winston GP, Micallef C, Kendell BE, et al. The value of repeat neuroimaging for epilepsy at a tertiary referral centre: 16 years of experience. *Epilepsy Res* 2013;105:349–55 CrossRef Medline
- Yagishita A, Arai N, Maehara T, et al. Focal cortical dysplasia: appearance on MR images. *Radiology* 1997;203:553–59 CrossRef Medline
- Jiang YJ, Ang LC, Blume WT. Extent of EEG epileptiform pattern distribution in “focal” cortical dysplasia. *J Clin Neurophysiol* 2010;27:309–11 CrossRef Medline
- Tassi L, Colombo N, Garbelli R, et al. Focal cortical dysplasia: neuropathological subtypes, EEG, neuroimaging and surgical outcome. *Brain* 2002;125(Pt 8):1719–32 Medline
- Thornton R, Vulliemoz S, Rodionov R, et al. Epileptic networks in focal cortical dysplasia revealed using electroencephalography-functional magnetic resonance imaging. *Ann Neurol* 2011;70:822–37 CrossRef Medline
- Hodozuka A, Tsuda H, Hashizume K, et al. Focal cortical dysplasia: pathophysiological approach. *Childs Nerv Syst* 2006;22:827–33 CrossRef Medline
- Besseling RMH, Jansen JFA, de Louw AJA, et al. Abnormal profiles of local functional connectivity proximal to focal cortical dysplasias. *PLoS One* 2016;11:e0166022 CrossRef Medline
- Chassoux F, Landré E, Mellerio C, et al. Type II focal cortical dysplasia: electroclinical phenotype and surgical outcome related to imaging. *Epilepsia* 2012;53:349–58 CrossRef Medline
- Hofman PAM, Fitt GJ, Harvey AS, et al. Bottom-of-sulcus dysplasia: imaging features. *AJR Am J Roentgenol* 2011;196:881–85 CrossRef Medline
- Zou QH, Zhu CZ, Yang Y, et al. An improved approach to detection of amplitude of low-frequency fluctuation (ALFF) for resting-state fMRI: fractional ALFF. *J Neurosci Methods* 2008;172:137–41 CrossRef Medline
- Zang YF, He Y, Zhu CZ, et al. Altered baseline brain activity in children with ADHD revealed by resting-state functional MRI. *Brain Dev* 2007;29:83–91 CrossRef Medline
- Wang Z, Zhang Z, Liao W, et al. Frequency-dependent amplitude alterations of resting-state spontaneous fluctuations in idiopathic generalized epilepsy. *Epilepsy Res* 2014;108:853–60 CrossRef Medline
- Zang Y, Jiang T, Lu Y, et al. Regional homogeneity approach to fMRI data analysis. *Neuroimage* 2004;22:394–400 CrossRef Medline
- Rosso OA. Entropy changes in brain function. *Int J Psychophysiol* 2007;64:75–80 CrossRef Medline
- Gupta L, Jansen JFA, Hofman PAM, et al. Wavelet entropy of BOLD time series: an application to Rolandic epilepsy. *J Magn Reson Imaging* 2017;46:1728–37 CrossRef Medline
- Menezes Cordeiro I, von Ellenrieder N, Zazubovits N, et al. Sleep influences the intracerebral EEG pattern of focal cortical dysplasia. *Epilepsy Res* 2015;113:132–39 CrossRef Medline
- Gotman J. Epileptic networks studied with EEG-fMRI. *Epilepsia* 2008;49(Suppl 3):42–51 CrossRef Medline
- Tassi L, Colombo N, Cossu M, et al. Electroclinical, MRI and neuropathological study of 10 patients with nodular heterotopia, with surgical outcomes. *Brain* 2005;128:321–37 Medline
- Palmini A, Gambardella A, Andermann F, et al. Intrinsic epileptogenicity of human dysplastic cortex as suggested by corticography and surgical results. *Ann Neurol* 1995;37:476–87 CrossRef Medline
- Urrestarazu E, Chander R, Dubeau F, et al. Interictal high-frequency oscillations (100–500 Hz) in the intracerebral EEG of epileptic patients. *Brain* 2007;130:2354–66 CrossRef Medline
- Cohen-Gadol AA, Ozduman K, Bronen RA, et al. Long-term outcome after epilepsy surgery for focal cortical dysplasia. *J Neurosurg* 2004;101:55–65 CrossRef Medline
- Hader WJ, Mackay M, Otsubo H, et al. Cortical dysplastic lesions in children with intractable epilepsy: role of complete resection. *J Neurosurg* 2004;100(2 Suppl Pediatrics):110–17 CrossRef Medline
- Alexandre V Jr, Walz R, Bianchin MM, et al. Seizure outcome after surgery for epilepsy due to focal cortical dysplastic lesions. *Seizure* 2006;15:420–27 CrossRef Medline
- Phi JH, Cho BK, Wang C, et al. Longitudinal analyses of the surgical outcomes of pediatric epilepsy patients with focal cortical dysplasia. *J Neurosurg Pediatr* 2010;6:49–56 CrossRef Medline
- Najm IM, Sarnat HB, Blümcke I. Review: the International Consensus Classification of Focal Cortical Dysplasia—a critical update 2018. *Neuropathol Appl Neurobiol* 2018;44:18–31 CrossRef Medline